Apparent activation energy in electrochemical multistep reactions: a description via Degrees of Rate Control

Alfredo Calderón-Cárdenas,[1,2,*] Enrique A. Paredes-Salazar,[1] Hamilton Varela[1,*]

[1] Instituto de Química de São Carlos, Universidade de São Paulo, CEP 13560-970, São Carlos-SP, Brazil
[2] GIFBA, Universidad de Nariño, ZIP Code 52001, San Juan de Pasto-Nariño, Colombia

* corresponding authors: hamiltonvarela@usp.br (HV), alfredocalderon@udenar.edu.co (ACC)

ABSTRACT

Activation energy is a well-known empirical parameter in chemical kinetics that characterizes the dependence of the chemical rate coefficients on the temperature and provides information to compare the intrinsic activity of the catalysts. However, the determination and interpretation of the apparent activation energy in multistep reactions is not an easy task. For this purpose, the concept of degree of rate control is convenient, which comprises a mathematical approach for analyzing reaction mechanisms and chemical kinetics. Although this concept has been used in catalysis, it has not yet been applied in electrocatalytic systems, whose ability to control the potential across the solid/liquid interface is the main difference with heterogenous catalysis, and the electrical current is commonly used as a measure of the reaction rate. Herein we use the definition of 'degree of rate control for elementary step' to address some of the drawbacks that frequently arise with interpreting apparent activation energy as a measure of intrinsic electrocatalytic activity of electrode. For this, an electrokinetic model Langmuir-Hinshelwood-like is used for making numerical experiments and verifying the proposed ideas. The results show that to improve the catalytic activity of an electrode material, it must act upon the reaction steps with the highest normalized absolute values of degree of rate control. On the other hand, experiments at different applied voltages showed that if the electroactive surface poisoning process take place, changes in E_{app} can not be used to compare the catalytic activity of the electrodes. Finally, the importance of making measurements at steady-state to avoid large errors in the calculations of apparent activation energy is also discussed.

Keywords: activation energy, degrees of rate control, electrochemical reactions, numerical simulations, electrocatalysis.

1. INTRODUCTION

The activation energy E_a is a well-known empirical parameter in chemical kinetics that characterizes the exponential dependence of the chemical rate coefficient on the temperature. According to the Arrhenius equation, the activation energy for an elementary reaction is defined as: [1]

$$E_a \equiv R\,T^2 \frac{d\ln k}{dT} \tag{1}$$

Where k is the rate coefficient, R is the gas constant, and T is the temperature. In addition to evaluating the effect of temperature on the reaction rate, the determination of activation energy is also important in catalysis because it provides information to compare the intrinsic activity of the catalysts since a better catalyst should supply lower activation energy.

Nevertheless, a chemical reaction can rarely be described by a single elementary step, and therefore, the definition of activation energy for multistep reactions needs to be rewritten as follow: [2]

$$E_{app} = R\,T^2 \frac{d\ln v}{dT} \tag{2}$$

Where v is the reaction rate, which can be defined as the disappearance rate of the reactants or the formation rate of products. Though the apparent activation energy E_{app} is commonly used instead of E_a, it must be carefully interpreted since, unlike to E_a, it is affected by experimental conditions such as pressure, concentration of reactants, and the same temperature. As a consequence, the Arrhenius plot, $\ln v$ *vs.* T^{-1}, may deviate from a straight line over a wide range of temperatures.[3] Furthermore, E_{app} is not constant over time and can vary until the system reaches a steady-state or quasi-steady-state, among other problems that hinder its interpretation, which will be discussed later. Therefore, a proper determination and interpretation of the activation energy in multistep reactions is not a trivial task.

In electrochemistry, if the contribution of non-Faradaic processes is disregarded, the current density $j(\phi,T)$ through the cell is a measure of the charge transfer rate across the electrode-solution interface. In the 1920s with the pioneering works of Bowden,[4] the activation energy for elementary electrochemical reactions was defined as:

$$E_a(\phi) \equiv R\,T^2 \left[\frac{\partial \ln j_F(\phi,T)}{\partial T}\right]_{\phi,C_R,P} \tag{3}$$

Where the derivative is taken at electrode potential ϕ, concentration of reagents C_R, and pressure P as constants. However, as with non-electrochemical reactions, most electrochemical processes are also not elemental. In this sense, for a multistep process, the apparent activation energy reads as: [5,6]

$$E_{app}(\phi) \equiv R\,T^2\left[\frac{\partial \ln j_{tot}(\phi,T)}{\partial T}\right]_{\phi,P} \tag{4}$$

Where $j_F(\phi,T)$ for a single chemical reaction is replaced by the total current density measured during the overall reaction $j_{tot}(\phi,T)$. Despite the interpretation problems for apparent activation energy above mentioned, $\ln j(\phi,T)$ *vs.* T^{-1} plots are often used to determine it.[7–9]

Recalling that, in electrochemistry, the activation energy is also a function of an electrical variable such as the cell voltage U measured respect to a reference electrode, the potential difference ϕ through the interface between the working electrode and the electrolytic solution (Galvani potential) or the overpotential η of the overall electrochemical reaction.[10] The choice of one of these variables determines the linear scale that governs the dependence of the activation energy with the chosen electric variable. In this manuscript, the E_a and E_{app} will be consider as a function of the potential difference ϕ for numerical convenience, and the obtained results are independent of the electric variable itself.

For elementary chemical reactions, whether chemical or electrochemical, E_{app} and E_a are identical; for multistep reactions, each step m has an activation energy $E_{a,m}$. For a proper interpretation of the apparent activation energy, an explicit relationship between E_{app} and $E_{a,m}$ must be determined. In order to do it, the concept of degree of rate control DRC [11] is very useful. As its name implies, the DRC evaluates the degree to which each reaction step contributes to the overall reaction rate. Among several formulations have been given for this concept to date,[12,13] herein we use the definition known as degree of rate control for elementary step $X_{RC,m}$:[12,14,15]

$$X_{RC,m} \equiv \frac{k_m}{\upsilon}\left(\frac{\partial \upsilon}{\partial k_m}\right)_{k_{n\neq m}} = \left(\frac{\partial \ln \upsilon}{\partial \ln k_m}\right)_{k_{n\neq m}} \tag{5}$$

Where υ is the net formation rate of a product of interest and the partial derivative is taken holding constant the forward and reverse rate coefficients $k_{\pm n}$ for all other steps $n \neq m$. $X_{RC,m}$ equals the relative change in the net reaction rate with respect to the relative increase in the rate coefficient of the step m. Using the concept of $X_{RC,m}$ and other related definitions, the relationship between E_{app} and $E_{a,m}$ has been derived for multistep chemical reactions.[16,17] This expression shows that apparent activation energy seems to a weighted

average of activation energy of each elementary step in the reaction mechanism, where each weight factor corresponding to $X_{RC,m}$,

$$E_{app}(\phi) = \sum_{m} X_{RC,m}\, E_{a,m} \tag{6}$$

Thus, $X_{RC,m}$ can be compared to the concept of rate-determining step RDS but in a much broader and more general way.[11,18,19] In this way, steps whose $X_{RC,m}$ values are positive are named rate-limiting steps, making it clear that there may be more than one RDS in certain mechanisms.[12,15] Steps where the degree of rate control is negative corresponds to inhibition ones, and finally, steps with $X_{RC,m}$ close to zero mean fast steps, *i.e.* those which do not limit the rate of the overall reaction. To our knowledge, the concept of DRC has not been applied to electrochemical reactions. In this paper, we take this task, define the $X_{RC,m}$ for an electrochemical system and interprete the apparent activation energy according to the contribution of individual steps. A prototype electrokinetic model including adsorption, surface reaction, and desorption has been used to accomplish this goal.

2. MODEL

The electrokinetic model consists of the adsorption of solution species A and B on free surface sites $*$, the reaction between these adsorbates in a Langmuir-Hinshelwood (LH) step, and the desorption of the product C:

$$\mathrm{A} + * \rightleftharpoons \mathrm{A_{ad}} + \mathrm{e^-} \quad (r1)$$

$$\mathrm{B} + * \rightleftharpoons \mathrm{B_{ad}} + \mathrm{e^-} \quad (r2)$$

$$\mathrm{A_{ad}} + \mathrm{B_{ad}} \rightleftharpoons \mathrm{C_{ad}} + * + \mathrm{e^-} \quad (r3)$$

$$\mathrm{C_{ad}} \rightleftharpoons \mathrm{C} + * \quad (r4)$$

This generic model keeps obvious resemblance with many (electro)chemical reactions.[7,20–25] In particular, step *r3* is ubiquitous in the electro-oxidation of small organic molecules as in the so-called Ertl reaction,[26] where adsorbed carbon monoxide CO_{ad} reacts with adsorbed oxygenated species $O(H)_{x,ad}$. The following rate laws can be written for each elementary reaction:

$$v_1 = k_1(\phi, T)\, C_A\, \theta_{vac} \quad (7)$$

$$v_{-1} = k_{-1}(\phi, T)\, \theta_A \quad (8)$$

$$v_2 = k_2(\phi, T)\, C_B\, \theta_{vac} \quad (9)$$

$$v_{-2} = k_{-2}(\phi, T)\, \theta_B \quad (10)$$

$$v_3 = k_3(\phi, T)\, \theta_A\, \theta_B \quad (11)$$

$$v_{-3} = k_{-3}(\phi, T)\, \theta_C\, \theta_{vac} \quad (12)$$

$$v_4 = k_4(T)\, \theta_C \quad (13)$$

$$v_{-4} = k_{-4}(T)\, C_C\, \theta_{vac} \quad (14)$$

Where v_m corresponds to the rate of each m-th single step in units of s^{-1}. C_A, C_B, and C_C are the concentrations of species A, B, and C in the electric double layer region, respectively. They are assumed to be constants and equal to the bulk concentrations, *i.e.* diffusion effects and other possible mass transport effects are neglected. θ_A, θ_B, and θ_C are the coverages of the adsorbed species A, B, and C, while $\theta_{vac} \equiv 1 - \theta_A - \theta_B - \theta_C$ is the fraction of vacant sites on the electrode surface.

Rate coefficients can be expressed by replacing the activation energy, which was defined according to electrode kinetics theory as $E_{a,m} = E_{a,m}^0 \mp \beta_m F\,(\phi - \phi^0)$,[4] in the Arrhenius equation:

$$k_{\pm m}(\phi, T) = A_m \, e^{-\frac{E_{a,m}^0 \mp \beta_m F (\phi - \phi^0)}{R T}} \quad (15)$$

where, A_m is the Arrhenius pre-exponential factor, $E_{a,m}^0$ is the standard activation energy of the m-th step reaction, F the Faraday constant, R the ideal gas constant, T the temperature, β_m is the charge transfer coefficient, which is assumed as 0.5 for all elementary reactions, and ϕ^0 is the potential difference in standard conditions. To decrease the number of unknown parameters, equation 15 can be rearranged by grouping the terms $E_{a,m}^0$ and ϕ^0 and expressed as:

$$k_{\pm m}(\phi, T) = A_m \, e^{-\frac{(E_{a,m}^0 \pm \beta_m F \phi^0) \mp \beta_m F \phi}{R T}} \quad (16)$$

For each reaction step indicated in equations *r1-r4*, typical numerical values for A_m and $\left(E_{a,m}^0 \pm \beta_m F \phi^0\right)$ were used and reported in Table I. Note that the reaction mechanism proposed here considers that the elementary reaction *r4* is not electrochemical. In such a way that the rate coefficients k_4 and k_{-4} do not depend on the potential being described by the classic Arrhenius equation:

$$k_{\pm m}(T) = A_m \, e^{-\frac{E_{a,m}}{R T}} \quad (17)$$

Table I: Values for the pre-exponential factors A_m and exponential parameters in equations 16 and 17. For reaction steps *r1*, *r2*, and *r3* the exponential parameters corresponding to $E_{a,m}^0 \pm \beta_m F \phi^0$, while for reaction step *r4*, it is $E_{a,m}$.

***m*-th reaction step**	**Pre-exponential factors**	**Exponential parameters / $kJ\ mol^{-1}$**
1	$10^8\ cm^3\ mol^{-1}\ s^{-1}$	39.5
-1	$10^8\ s^{-1}$	22.0
2	$10^8\ cm^3\ mol^{-1}\ s^{-1}$	40.0
-2	$10^8\ s^{-1}$	25.0
3	$10^8\ s^{-1}$	80.0
-3	$10^8\ s^{-1}$	15.0
4	$10^8\ s^{-1}$	55.0
-4	$10^8\ cm^3\ mol^{-1}\ s^{-1}$	40.0

The electrokinetic model is defined by the electric charge balance and the mass balances of the chemical species on the electrode surface in terms of θ_A, θ_B, and θ_C, as it has

been presented and explained in other electrokinetic systems.[25,27–29] The core model consists of the equations:

$$\frac{d\theta_A}{dt} = v_1 - v_{-1} - v_3 + v_{-3} \tag{18}$$

$$\frac{d\theta_B}{dt} = v_2 - v_{-2} - v_3 + v_{-3} \tag{19}$$

$$\frac{d\theta_C}{dt} = v_3 - v_{-3} - v_4 + v_{-4} \tag{20}$$

$$C_d \frac{d\phi}{dt} = \frac{U - \phi}{A\, R_s} - F\, N_{tot}\, (v_1 - v_{-1} + v_2 - v_{-2} + v_3 - v_{-3}) \tag{21}$$

Where C_d is the capacitance associated with the electric double layer, A is the electroactive area, R_s is the electrical resistance between the reference and working electrodes, and N_{tot} is the total number of electroactive sites at the electrode surface. Equation 21 considers that the overall current density $j(\phi, T)$ is the sum of capacitive and Faradaic currents of each reaction step.

This model simulates the electrochemical response of a system in chronoamperometric experiments using the standard hydrogen electrode SHE as reference electrode. The coverage of adsorbates was determined after setting the voltage $U = 0\ V$ for 300 s with initial conditions of $\theta_A = \theta_B = \theta_C = \phi = 0$. The coverages reached were used as new initial experimental conditions when applying the potential step to the desired voltage. Table II shows the values of the constant terms used for the numerical integration of the set of ordinary differential equations 18-21, for which was used the software Wolfram Research, Inc., Mathematica version 12.1, Champaign, IL (2020). All additional numerical calculations, *e.g.* $X_{RC,m}$ determination by varying the rate coefficients values and calculating the resulting increase in the overall rate, were also carried out with this software.

Table II: Values of the constant terms used in the numerical integration of equations 18-21.

Constants values used in the numerical experiments	
$C_A\ /\ mol\ cm^{-3}$	1.0 x10^{-4}
$C_B\ /\ mol\ cm^{-3}$	1.0 x10^{-4}
$C_C\ /\ mol\ cm^{-3}$	0.00
$C_d\ /\ C\ V^{-1}\ cm^{-2}$	1.0 x10^{-6}
$N_{tot}\ /\ mol\ cm^{-2}$	1.0 x10^{-9}
$R_s\ /\ \Omega$	1.00
$A\ /\ cm^2$	1.00

3. RESULTS AND DISCUSSION

According to equation 6, when there is a single RDS in the reaction mechanism, then $X_{RC,m=RDS} \rightarrow 1$ for this step and $X_{RC,m\neq RDS} \rightarrow 0$ for all other steps.[15] In this situation, $E_{app} \approx E_{a,m=RDS}$ and apparent activation energy keeps the same interpretation of E_a, *i.e.* E_{app} characterizes the temperature dependence of the rate coefficients and the intrinsic activity of the catalyst. Nevertheless, interpretation problems for E_{app} appear in multistep reactions. Some of these situations will be discussed in the following using the described electrochemical model.

3.1. Multiple RDS in the reaction mechanism and inhibition process

Figure 1 shows some diagrams of Gibbs energy. The horizontal lines represent the relative Gibbs energy of reactants (A and B), intermediates (A^*, B^*, and C^*), products (C), and chemical species in their corresponding transition states ($TS1$, $TS2$, $TS3$, and $TS4$) at different potentials. The diagrams were made considering linear dependence of the activation energies with ϕ, according to the exponential terms in equation 16 and the values reported in Table I, where the activation energies are the difference between the energy of the transition state and the energy of the reactants in the corresponding reaction step.

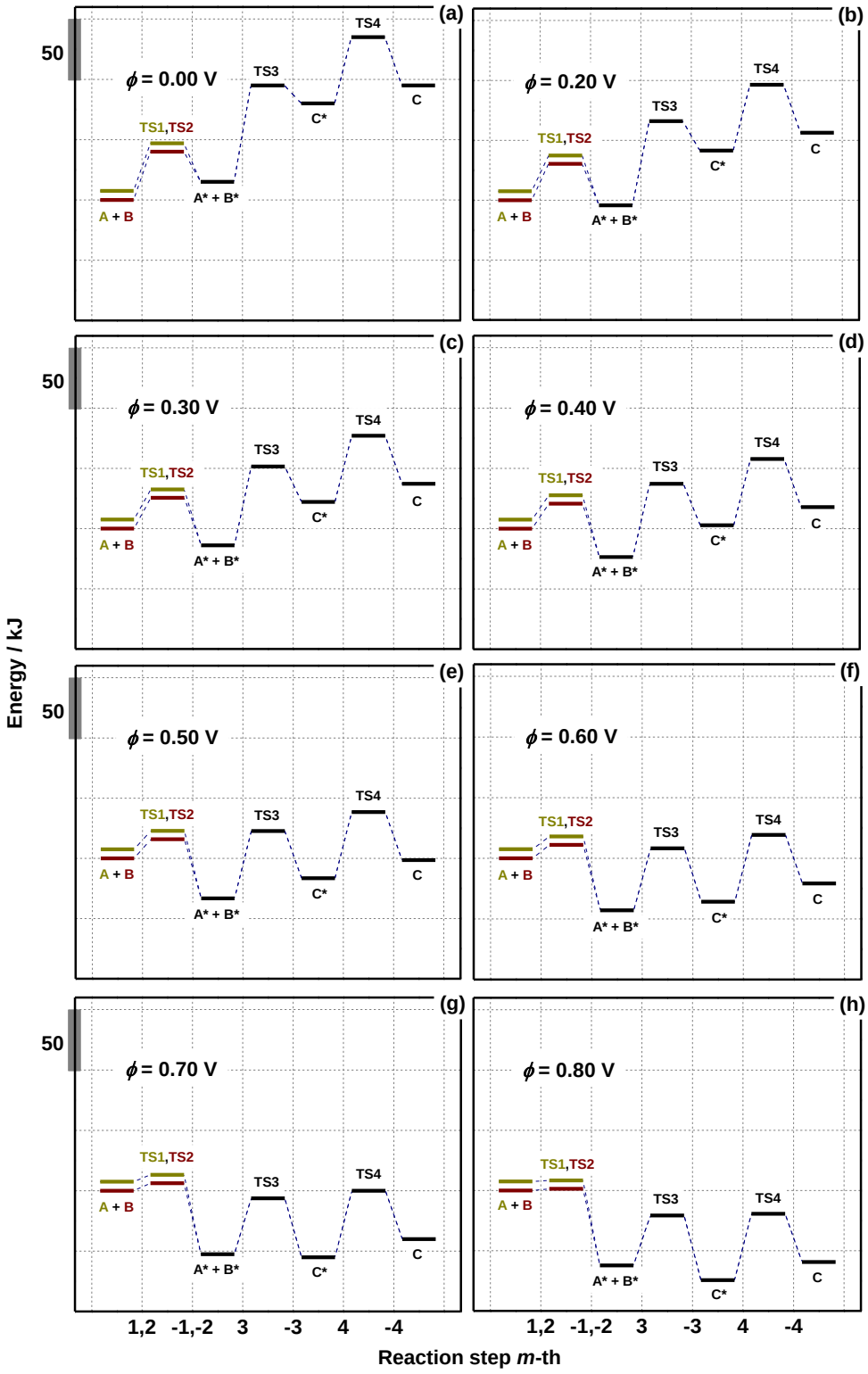

Figure 1: Diagrams of relative energies between reactants (A and B), intermediates (A^*, B^*, and C^*), product (C), and transitions states ($TS1$, $TS2$, $TS3$, and $TS4$) for the electrochemical process considered in this work at different potentials ϕ.

When $\phi = 0$, the energy diagram corresponding to the reaction in the charge-free state of the interface, Figure 1(a). From the classical perspective, the RDS is the step in the mechanism in which the reaction passes over the highest energy in the overall energy landscape.[30] Here, reaction step 3 has the highest activation energy among the three reaction steps of our process, in the left to right direction. Nevertheless, from the perspective of the analysis using the degrees of rate control,[15] this reaction step is not much greater than activation energies of steps 4, 2, or 1 and it is inappropriate to consider *a priori* that reaction step 3 is the single RDS because all reaction steps seem to significantly influence the overall rate of the reaction. Thus, all steps 1, 2, 3, and 4 could, in principle, affect the reaction rate.

The increase in the potential ϕ implies the decrease of the activation energies of all electro-oxidation steps and the increase of the activation energies of the reverse ones. Thus, in our electrokinetic model, the increase in potential leads to a decrease in the numerical difference between the values of $E_{a,m}$, except steps 1 and 2, which significantly decrease their activation energy compared to the other steps. It should be noted that in these cases it is even much more difficult to determine a single RDS. In order to determine the contribution of each reaction step to the overall rate, it is required to redefine the degree of rate control $X_{RC,m}$ for electrochemical reactions in which the global reaction rate v is replaced by the total current density $j(\phi, T)$.

$$X_{RC,m}(\phi, T) \equiv \left[\frac{\partial \ln j(\phi, T)}{\partial \ln k_m}\right]_{k_{n\neq m}} \tag{22}$$

Figure 2(a) shows the applied voltage profile and electrode potential ϕ as dynamic response of the system, while Figure 2(c) shows the variation of the other dynamic variables of the system, *i.e.* the time response of θ_A, θ_B, and θ_C. Note that at $U = 0.50\ V$, the formation of absorbed species A is faster than B and C, *i.e.* θ_A is more favored than θ_B and θ_C. Regarding the current density profile, it can be seen in Figure 2(b) that reaction steps 1 and 2 have the highest Faradaic currents $j_{F,m}$ among oxidations reactions, while steps -3 and -2 contribute to the highest Faraday reduction currents. Figure 2(d) shows the values of $X_{RC,m}$ as time function calculated by equation 22 during the numerical chronoamperometric experiment. For the calculation of each $X_{RC,m}$, equations 5 and 22 (non-electrochemical and electrochemical reactions, respectively) require the performance of several numerical experiments at different values k_m in order to determine the corresponding derivatives.

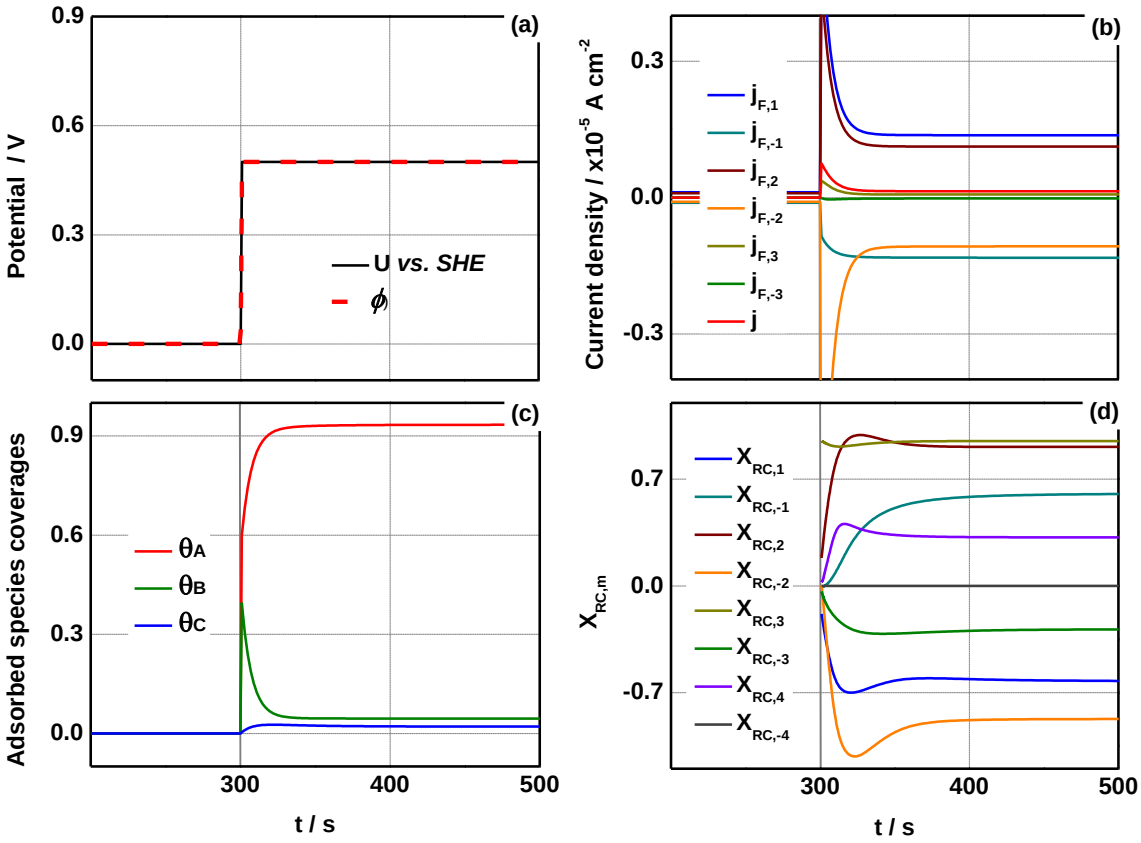

Figure 2: Numerical results of the chronoamperometric experiments at $U = 0.50\ V\ vs. SHE$. (a) Applied voltage U step from $0.00\ V$ to $0.50\ V$ and electrode potential ϕ as dynamic response of the system; (b) Total and Faradaic current density profiles of individual reaction step; (c)Time-evolution coverages of θ_A, θ_B, and θ_C, and (d) Degrees of rate control $X_{RC,m}$.

Table III presents a summary of the $X_{RC,m}$ and activation energies values for each reaction step determined at $t = 900\ s$, that is, $600\ s$ after applying the potential step from $0.00\ V$ to $0.50\ V$. This value is chosen by seeking steady-state conditions where $\sum_m X_{RC,m} = 1$.[12,18,31] Therefore, using the $X_{RC,m}$ and $E_{a,m}$ values in equation 6, the apparent activation energy $E_{app} = 55.36\ kJ\ mol^{-1}$ was determined at $U = 0.50\ V$, which is compared with $E_{app} = 55.34\ kJ\ mol^{-1}$ determined with an Arrhenius-like curve (equation 4). The similarity between these two values demonstrates the validity of equation 6.

Table III: $X_{RC,m}$, $E_{a,m}$, and *normalized contribution (NC) to* E_{app} for each reaction step determined at steady-state conditions at $U = 0.50\ V\ vs. SHE$.

***m*-th reaction step**	$X_{RC,m}$	$E_{a,m}$ / $kJ\ mol^{-1}$	***Normalized contribution to*** E_{app}
1	-0.627	15.379	0.137
-1	0.606	56.121	0.133
2	0.912	15.879	0.200
-2	-0.874	49.121	0.191
3	0.949	55.879	0.208
-3	-0.283	39.121	0.062
4	0.318	55.000	0.070
-4	0.000	40.000	0.000

In order to estimate the individual contributions of elementary steps to E_{app}, the $X_{RC,m}$ absolute values were normalized. Thus, it is possible to deduce that steps 3, 2, -1 and 4 positively contribute to the total value of E_{app} with 20.8%, 20.0%, 13.3%, and 7.0%, respectively. While the $X_{RC,m}$ for the inhibition reaction steps -2, 1, and -3 negatively contribute to the E_{app} with 19.1%, 13.7%, and 6.2%, respectively. Finally, the reaction step -4 does not limit the overall rate reaction, which is reasonable since we have considered that the concentration of C is constant and equal to zero. These results serve as an example to propose the normalization of $X_{RC,m}$ absolute values as a feasible way to quantify the relative contribution of each reaction step to the overall reaction rate.

On the other hand, it is to be expected that the reverse steps, in the direction $C \rightarrow A + B$, act as steps of inhibition against the formation of product C and contributing with negative $j_{F,m}$ (Figure 2(b)), according to the agreement that positive currents correspond to electro-oxidation processes. However, steps 1 and -1 follow an apparently anomalous behavior because the inhibition process is due to the forward step instead of the backward step. In Figure 2(c) it can be seen that at the applied voltage $U = 0.50\ V$, the coverage of adsorbed species A is greater than 0.90 while the coverage of B is less than 0.10. The meaning of the negative sign for $X_{RC,1}$ and the positive sign for $X_{RC,-1}$ is that by increasing the reaction rate of step 1 in the forward direction, the coverage of A limits the adsorption of B, decreasing the current density of the global reaction. In this sense, the decrease in the activation energy for a reaction step which blocks the electroactive sites, *e.g.* step *r1* in this case, will cause a global increase in the E_{app}.

Therefore, in order to improve the catalytic activity of an electrode material, it must act upon the reaction steps with the highest NC. In such a way that the activation energy of the RDS is decreased and slightly increasing the activation energy of the steps that block the catalytic surface.

3.2. Dependency of the apparent activation energy with the applied voltage

So far, the results for $U = 0.50\ V$ have been discussed. Figure 3 shows the results of the simulated chronoamperometries at $U = 0.60\ V$, $0.70\ V$, and $0.80\ V\ vs. SHE$.

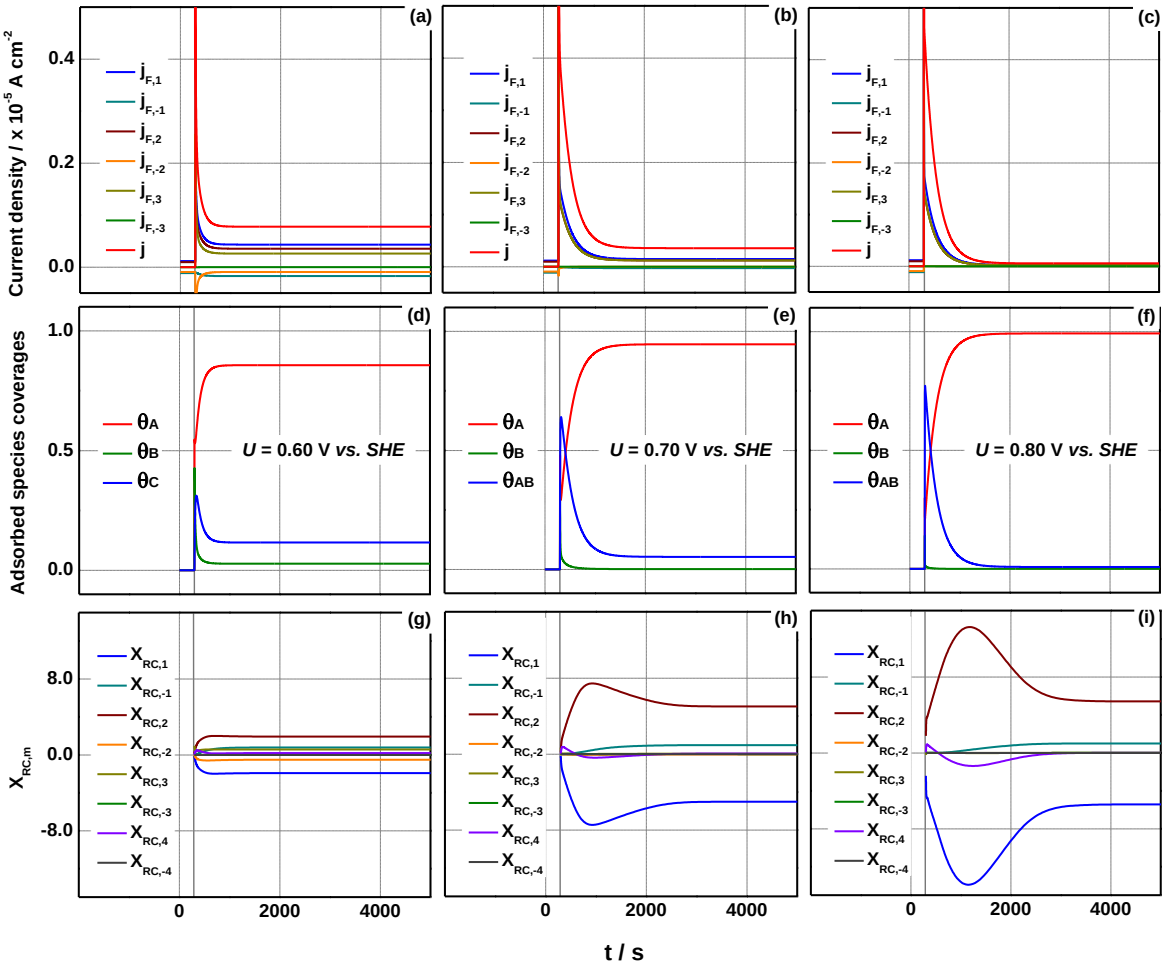

Figure 3: Time-evolution of the current density of individual steps at (a) $0.60\ V$, (b) 0.70 V, (c) $0.80\ V$; of coverages θ_A, θ_B, and θ_{AB} at (d) $0.60\ V$, (e) $0.70\ V$, (f) $0.80\ V$; and of $X_{RC,m}$ (g) $0.60\ V$, (h) $0.70\ V$, (i) $0.80\ V$.

It is to be expected that by increasing the applied voltage, the rate of the electro-oxidation steps is increased and in turn the rate of the backward reactions is slowed down, *cf.* equation 16. As consequence the total current density should increase. However, in Figure 3 can be seen that $j(\phi, T)$ decreases with U because the blockage of the electrode surface by species A becomes more important, as has been discussed above. Note that at $0.80\ V$, θ_A is close to 1 while θ_B and θ_{AB} are almost 0. This coverage has an important effect on the voltammetric profile [32] as can be seen in Figure 4 which shows $j(\phi, T)$ and E_{app} in steady-state conditions as a function of U.

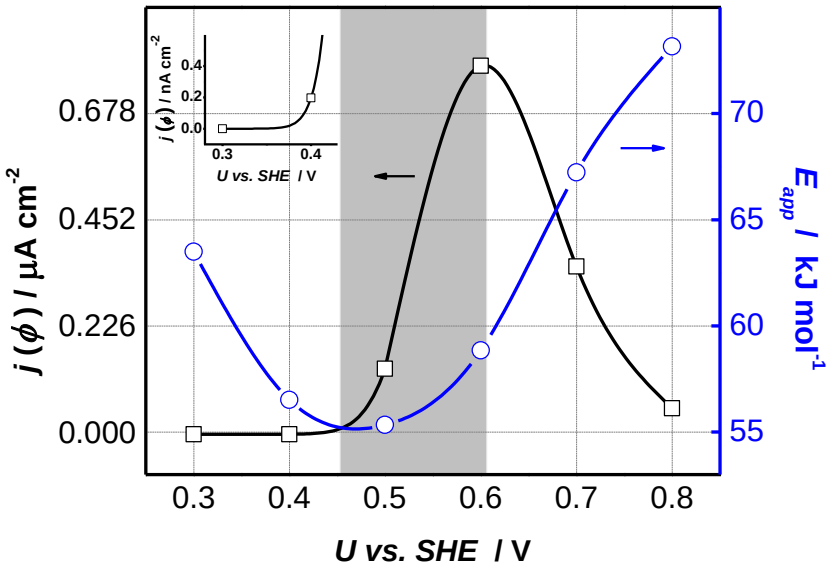

Figure 4: $j(\phi, T)$ and E_{app} calculated at $t = 4000\ s$ after the potential step as a function of the applied voltage.

When the applied voltage increases from $0.30\ V$ to approximately $0.45\ V$, the E_{app} decreases and $j(\phi, T)$ increases, suggesting an inverse relationship between the two parameters, as expected. After $0.60\ V$, E_{app} and $j(\phi, T)$ also have an inverse behavior, but contrary to the first case, $j(\phi, T)$ decreases with increasing U. This is a widely documented behavior in various articles that address the study of complex dynamics in electrocatalytic reactions [33,34,35] and is associated with the previously described reaction inhibition processes.

However, an outstanding behavior between E_{app} and $j(\phi, T)$ is observed in the range of potentials from $0.45\ V$ to $0.60\ V$, in which both E_{app} and $j(\phi, T)$ increases. Although the electroactive surface poisoning process is already happening in this potential range, with species A as the main electrocatalytic poison, this is an electro-oxidation process that contributes to the total current density continuing to increase. This situation is characteristic of electrochemical systems that present a hidden negative differential resistance during the reaction dynamics, such as the oxidation of low molecular mass organic molecules.[33,36,37] Thus, a decrease in the activation energy of the processes of inhibition by voltage increase, *e.g.* the steps of formation of catalytic poisons, leads to an increase in the value of E_{app} as was discussed in the previous section, affecting the expected inverse behavior between E_{app} and $j(\phi, T)$.

Therefore, if the increase in the reaction rate does not imply a lower apparent activation, the role of E_{app} as a parameter that allows comparing the intrinsic activity of catalysts in an electrochemical process abruptly fails. These results suggest that the apparent

activation energy is not useful for the mentioned purpose in any electrocatalytic reaction when it involves the formation of species that block the electroactive surface.

3.3. Determination of the apparent activation energy under non-stationary conditions

A comparison of Figures 2(d), 3(g), 3(h), and 3(i) reveals for higher applied voltages, the integration time in the numerical experiments to reach the steady-state considerably increase. The time evolution of $X_{RC,m}$ after applying the potential step suggests that E_{app} will also change in time until reaching the steady-state according to equation 6. It is worth noting that the activation energies of the elementary steps are constant during the transient, since $E_{a,m}$ are only functions of the potential ϕ, that remains constant because of $U \approx \phi$, *cf.* Figure 2(a).

To analyze the behavior of the apparent activation energy during the transient, Figure 4 shows the E_{app} values calculated at $U = 0.70\ V$ at different reaction times after applying the potential step in the chronoamperometric experiment. The apparent activation energy also was calculated using an Arrhenius-like curve for comparison purposes.

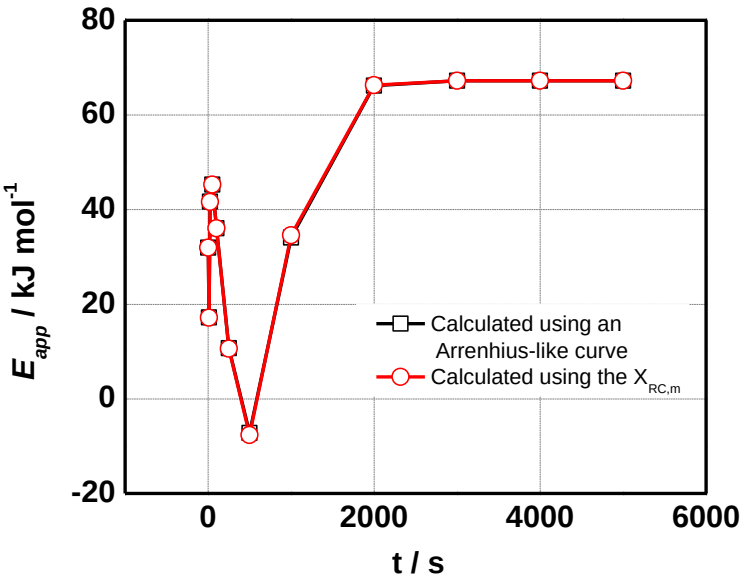

Figure 5: Time-evolution of E_{app} after applying the potential step from $0.00\ V$ to $0.70\ V\ vs. SHE$, calculated using the $X_{RC,m}$ and by an Arrhenius-like curve, *cf.* equations 4 and 6.

The time evolution of E_{app} shows alternate and abrupt changes before reaching steady-state, even taking negative values for apparent activation energy at times around $500\ s$. Hence, apparent activation energy determinations using current values at short

reaction times can lead to large errors due to the enormous variations of the $X_{RC,m}$ during the transient. These results highlight the importance of guaranteeing steady-state conditions for apparent activation energy determinations, both for numerical calculations and experimental measurements. The results also suggest that experimental determinations of E_{app} by voltammetry or other electrodynamic techniques are not suitable. Therefore, the interpretation of the E_{app} as a descriptor of the intrinsic catalytic activity is even less adequate than in the cases described in the previous sections.

Finally, it is worth mentioning that in multistep electrochemical reactions, approaches based on the different definitions of DRC, adapted to electrocatalytic systems, may be more suitable to compare the catalytic activity of electrode materials.

4. CONCLUSIONS

We have employed a generic electrochemical model to study the relationship between apparent activation energy and the activation energies of the elementary reaction steps, which includes steps commonly found in electrocatalytic systems, *viz.* some fuel cells relevant reactions. Using the concept of degree of rate control, which we defined in terms of current density, it was showed that to improve the catalytic activity of an electrode material, it must act upon the reaction steps with the highest normalized absolute values of $X_{RC,m}$. In such way that i) it decreases the activation energy of the rate-determining steps; and ii) slightly increases the activation energy of the steps that block the catalytic surface. On the other hand, it was observed the importance of guaranteeing steady-state conditions to avoid large errors in the calculations of apparent activation energy. It suggests that experimental determinations of E_{app} by voltammetry or other electrodynamic techniques may not be suitable.

Finally, numerical experiments at different applied voltages showed that if the electroactive surface poisoning process take place, an increase in the total current density does not imply a decrease in the apparent activation energy. Therefore, changes in E_{app} can not be used to compare the catalytic activity of the electrodes. For these purposes, the comparison of the activation energies of each reaction step or approaches based on the concept of degree of rate control adapted to electrocatalytic systems, are more appropriate to compare the catalytic activity of electrode materials in multistep reactions.

5. ACKNOWLEDGMENTS

H.V. acknowledges São Paulo Research Foundation (FAPESP) for the financial support (#2013/16930-7). H.V. acknowledges Conselho Nacional de Desenvolvimento Científico e Tecnológico (CNPq) for financial support (#306060/2017-5). This study was financed in part by the Coordenação de Aperfeiçoamento de Pessoal de Nível Superior – Brasil (CAPES) – Finance Code 001.

6. REFERENCES

(1) Cohen, E. R.; Cvitas, T.; Frey, J. G. F.; Holmström, B.; Kuchitsu, K.; Marquardt, R.; Mills, I.; Pavese, F.; Quack, M.; Stohner, J.; Strauss, H. L.; Takami, M.; Thor, A. J. *Quantities, Units and Symbols in Physical Chemistry*, 3 Edition.; IUPAC, Ed.; RSC Publishing: Cambridge, 2007.

(2) Chorkendorff, I.; Niemantsverdriet, J. W. *Concepts of Modern Catalysis and Kinetics*; Wiley-VCH Verlag GmbH & Co. KGaA: Weinheim, 2003.

(3) Jensen, F. Activation Energies and the Arrhenius Equation. *Qual. Reliab. Eng. Int.* **1985**, *1* (1), 13–17. https://doi.org/10.1002/qre.4680010104.

(4) Bowden, F. P. The Kinetics of the Electro-Deposition of Hydrogen and Oxygen. *Proc. R. Soc. London. Ser. A, Contain. Pap. a Math. Phys. Character* **1929**, *126* (800), 107–125. https://doi.org/10.1098/rspa.1929.0207.

(5) Angelucci, C. A.; Varela, H.; Herrero, E.; Feliu, J. M. Activation Energies of the Electrooxidation of Formic Acid on Pt(100). *J. Phys. Chem. C* **2009**, *113* (43), 18835–18841. https://doi.org/10.1021/jp907723k.

(6) Nagao, R.; Epstein, I. R.; Gonzalez, E. R.; Varela, H. Temperature (over)Compensation in an Oscillatory Surface Reaction. *J. Phys. Chem. A* **2008**, *112* (20), 4617–4624. https://doi.org/10.1021/jp801361j.

(7) Hartl, F. W.; Zülke, A. A.; Fonte, B. J.; Varela, H. Temperature Dependence of the Evolving Oscillations along the Electrocatalytic Oxidation of Methanol. *J. Electroanal. Chem.* **2017**, *800*, 99–105. https://doi.org/10.1016/j.jelechem.2016.11.032.

(8) Perales-Rondón, J. V.; Herrero, E.; Feliu, J. M. On the Activation Energy of the Formic Acid Oxidation Reaction on Platinum Electrodes. *J. Electroanal. Chem.* **2015**, *742*, 90–96. https://doi.org/10.1016/j.jelechem.2015.02.003.

(9) Camargo, A. P. M.; Previdello, B. A. F.; Varela, H.; Gonzalez, E. R. Effect of Temperature on the Electro-Oxidation of Ethanol on Platinum. *Quim. Nova* **2010**, *33* (10), 2143–2147. https://doi.org/10.1590/S0100-40422010001000026.

(10) Sepa, D. B. Energies of Activation of Electrode Reactions: A Revisited Problem. In *Modern aspects of electrochemistry 29*; Bockris, J. O., Conway, B. E., White, R. E., Eds.; Plenum Press: New York, 1996; pp 1–56. https://doi.org/10.1007/978-1-4613-0327-5.

(11) Campbell, C. T. The Degree of Rate Control: A Powerful Tool for Catalysis Research. *ACS Catal.* **2017**, *7* (4), 2770–2779. https://doi.org/10.1021/acscatal.7b00115.

(12) Stegelmann, C.; Andreasen, A.; Campbell, C. T. Degree of Rate Control: How Much the Energies of Intermediates and Transition States Control Rates. *J. Am. Chem. Soc.* **2009**, *131* (23), 8077–8082. https://doi.org/10.1021/ja9000097.

(13) Norskov, J. K.; Bligaard, T.; Kleis, J. Rate Control and Reaction Engineering. *Science (80-.).* **2009**, *324* (5935), 1655–1656. https://doi.org/10.1126/science.1174885.

(14) Laidler, K. J. Rate Controlling Step: A Necessary or Useful Concept? *J. Chem. Educ.* **1988**, *65* (3), 250. https://doi.org/10.1021/ed065p250.

(15) Campbell, C. T. Future Directions and Industrial Perspectives Micro- and Macro-

Kinetics: Their Relationship in Heterogeneous Catalysis. *Top. Catal.* **1994**, *1* (3–4), 353–366. https://doi.org/10.1007/BF01492288.

(16) Meskine, H.; Matera, S.; Scheffler, M.; Reuter, K.; Metiu, H. Examination of the Concept of Degree of Rate Control by First-Principles Kinetic Monte Carlo Simulations. *Surf. Sci.* **2009**, *603* (10–12), 1724–1730. https://doi.org/10.1016/j.susc.2008.08.036.

(17) Mao, Z.; Campbell, C. T. Apparent Activation Energies in Complex Reaction Mechanisms: A Simple Relationship via Degrees of Rate Control. *ACS Catal.* **2019**, *9* (10), 9465–9473. https://doi.org/10.1021/acscatal.9b02761.

(18) Campbell, C. T. Finding the Rate-Determining Step in a Mechanism. *J. Catal.* **2001**, *204* (2), 520–524. https://doi.org/10.1006/jcat.2001.3396.

(19) Baranski, A. On the Usefulness of Campbell's Concept of the Rate-Determining Step. *Solid State Ionics* **1999**, *117* (1–2), 123–128. https://doi.org/10.1016/S0167-2738(98)00255-0.

(20) Silva, M. F.; Delmonde, M. V. F.; Batista, B. C.; Boscheto, E.; Varela, H.; Camara, G. A. Oscillatory Electro-Oxidation of Ethanol on Platinum Studied by in Situ ATR-SEIRAS. *Electrochim. Acta* **2019**, *293*, 166–173. https://doi.org/10.1016/j.electacta.2018.10.019.

(21) Ferreira, G. C. A.; Napporn, T. W.; Kokoh, K. B.; Varela, H. Complex Oscillatory Kinetics in the Electro-Oxidation of Glucose on Gold. *J. Electrochem. Soc.* **2017**, *164* (9), H603–H607. https://doi.org/10.1149/2.072179jes.

(22) Zülke, A.; Perroni, P.; Machado, E. G.; Varela, H. Rrde Studies of Glycerol Electro-Oxidation: Local PH Variation and Oscillatory Dynamics. *ECS Trans.* **2017**, *77* (11), 1643–1650. https://doi.org/10.1149/07711.1643ecst.

(23) Calderón-Cárdenas, A.; Ortiz-Restrepo, J. E.; Mancilla-Valencia, N. D.; Torres-Rodriguez, G. A.; Lima, F. H. B.; Bolaños-Rivera, A.; Gonzalez, E. R.; Lizcano-Valbuena, W. H. CO and Ethanol Electro-Oxidation on Pt-Rh/C. *J. Braz. Chem. Soc.* **2014**, *25* (8), 1391–1398. https://doi.org/10.5935/0103-5053.20140121.

(24) Ocampo-Restrepo, V. K.; Calderón-Cárdenas, A.; Lizcano-Valbuena, W. H. Catalytic Activity of Pt-Based Nanoparticles with Ni and Co for Ethanol and Acetaldehyde Electrooxidation in Alkaline Medium. *Electrochim. Acta* **2017**, *246*, 475–483. https://doi.org/10.1016/j.electacta.2017.06.014.

(25) Calderón-Cárdenas, A.; Hartl, F. W.; Gallas, J. A. C.; Varela, H. Modeling the Triple-Path Electro-Oxidation of Formic Acid on Platinum: Cyclic Voltammetry and Oscillations. *Catal. Today* **2020**, (In press). https://doi.org/10.1016/j.cattod.2019.04.054.

(26) Ertl, G. Reactions at Surfaces: From Atoms to Complexity (Nobel Lecture). *Angew. Chemie - Int. Ed.* **2008**, *47* (19), 3524–3535. https://doi.org/10.1002/anie.200800480.

(27) Freire, J. G.; Calderón-Cárdenas, A.; Varela, H.; Gallas, J. A. C. Phase Diagrams and Dynamical Evolution of the Triple-Pathway Electro-Oxidation of Formic Acid on Platinum. *Phys. Chem. Chem. Phys.* **2020**, *22* (3), 1078–1091. https://doi.org/10.1039/C9CP04324A.

(28) Mei, D.; He, Z.-D.; Jiang, D. C.; Cai, J.; Chen, Y. Modeling of Potential Oscillation during Galvanostatic Electrooxidation of Formic Acid at Platinum Electrode. *J. Phys. Chem. C* **2014**, *118* (12), 6335–6343. https://doi.org/10.1021/jp500285j.

(29) Mukouyama, Y.; Kikuchi, M.; Samjeské, G.; Osawa, M.; Okamoto, H. Potential

Oscillations in Galvanostatic Electrooxidation of Formic Acid on Platinum: A Mathematical Modeling and Simulation. *J. Phys. Chem. B* **2006**, *110* (24), 11912–11917. https://doi.org/10.1021/jp061129j.

(30) Koper, M. T. M. Analysis of Electrocatalytic Reaction Schemes: Distinction between Rate-Determining and Potential-Determining Steps. *J. Solid State Electrochem.* **2013**, *17* (2), 339–344. https://doi.org/10.1007/s10008-012-1918-x.

(31) Foley, B. L.; Bhan, A. Degrees of Rate Control at Non(Pseudo)Steady-State Conditions. *ACS Catal.* **2020**, *10* (4), 2556–2564. https://doi.org/10.1021/acscatal.9b04910.

(32) Okamoto, H.; Kon, W.; Mukouyama, Y. Stationary Voltammogram for Oxidation of Formic Acid on Polycrystalline Platinum. *J. Phys. Chem. B* **2004**, *108* (14), 4432–4438. https://doi.org/10.1021/jp031052o.

(33) Varela, H.; Delmonde, M. V. F.; Zülke, A. A. The Oscillatory Electrooxidation of Small Organic Molecules. In *Electrocatalysts for Low Temperature Fuel Cells: Fundamentals and Recent Trends*; Maiyalagan, T., Saji, V. S., Eds.; Wiley-VCH Verlag GmbH & Co. KGaA: Weinheim, 2017; pp 145–163. https://doi.org/10.1002/9783527803873.ch5.

(34) Zülke, A. A.; Varela, H. The Effect of Temperature on the Coupled Slow and Fast Dynamics of an Electrochemical Oscillator. *Sci. Rep.* **2016**, *6* (1), 24553. https://doi.org/10.1038/srep24553.

(35) Hartl, F. W.; Varela, H. The Effect of Solution pH and Temperature on the Oscillatory Electro-Oxidation of Formic Acid on Platinum. *ChemistrySelect* **2017**, *2* (27), 8679–8685. https://doi.org/10.1002/slct.201702008.

(36) Delmonde, M. V. F.; Nascimento, M. A.; Nagao, R.; Cantane, D. A.; Lima, F. H. B.; Varela, H. Production of Volatile Species during the Oscillatory Electro-Oxidation of Small Organic Molecules. *J. Phys. Chem. C* **2014**, *118* (31), 17699–17709. https://doi.org/10.1021/jp5044915.

(37) Gojuki, T.; Numata, Y.; Mukouyama, Y.; Okamoto, H. Hidden Negative Differential Resistance in the Oxidation of Formic Acid on Platinum. *Electrochim. Acta* **2014**, *129*, 142–151. https://doi.org/10.1016/j.electacta.2014.02.102.